

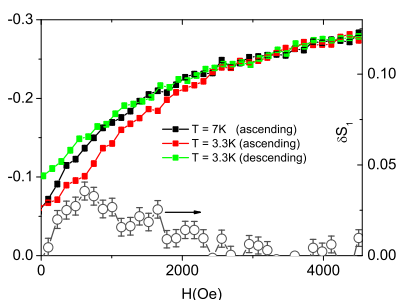
Student's name: Joel Gironés Domínguez
 Supervisor's name: Mrs. Vladimir. D. Zhaketov
 International Remote Student Training at JNIR

Superconductivity and Ferromagnetism Coexistence and Neutron Measurements

Introduction

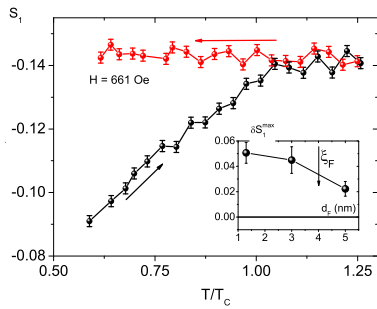
It has been known that the behavior of superconductors and ferromagnets at the magnetic field are the opposite. The Superconductor displaces the magnetic field because of the Meissner effect. In the case of the ferromagnet, it can fully penetrate. The thickness of the layers of low-dimensional heterostructures is about 1-100 nm, which corresponds to the known solid-state physics's known correlation lengths. So, at the superconducting/ferromagnetic heterostructures, the existence of intriguing proximity effects is possible because of the interaction and interpenetration of these two order parameters. However, the effects are not possible at the bulk materials. In order to understand this a little bit better, let us analyze three different structures. On the one hand, the superconducting order parameter can change the magnetic parameters of the structure. This is the case when studying the magnetic and superconductive properties of superlattices of composition $[\text{Gd}(d_F)/\text{Nb}(25 \text{ nm})]_{12}$ that were deposited on $25 \times 25 \text{ mm}^2$ $(1102)\text{Al}_2^{-1}\text{O}_3$ substrates and covered by an Nb (5nm) capping layer. Later on, it was cut into $\sim 5 \times 5 \text{ mm}^2$ pieces for magnetization and transport measurements. There were created different configurations that are described in three different samples. The thickness of the Gd layers was chosen to be $d_f = 0.5\xi_F$ (sample 1), $0.75\xi_F$ (sample 2), and $1.25\xi_F$ (sample 3). When studying these structures, interesting results came out. In order to understand this better, let us analyze the field and temperature behavior of the spin asymmetry at the first Bragg peak S_1 .

Above T_c , the following protocol was used. First, the sample was magnetized for a short time in the maximum magnetic field $H_{\text{max}} = 4.5 \text{ kOe}$. Then the field was released to zero, and $S_1(H)$ was measured for ascending magnetic field from 50e to H_{max} [Which can be seen in the black curve from the following figure].



Then the field was released to zero, and the sample was cooled down to $T = 3.3 \text{ K}$ in zero magnetic field. After, it was repeated $S_1(H)$ by first raising the magnetic field from 50e to H_{max} [red curve] and then lowering it to $H=50\text{e}$ [green curve].

The $S_1(H)$ curve above T_c repeats qualitatively the behavior of the upper branch of the macroscopic magnetic moment: The $S_1(H)$ curve grows from remanence to $H \sim 2\text{kOe}$ and then approaches saturation, which supports the used experimental logic. The corresponding curve below T_c is somewhat suppressed in the range of fields between remanence and saturation. The suppression is maximal around $H \approx 700\text{Oe}$. The descending curve, in turn, is different in small fields close to zero.

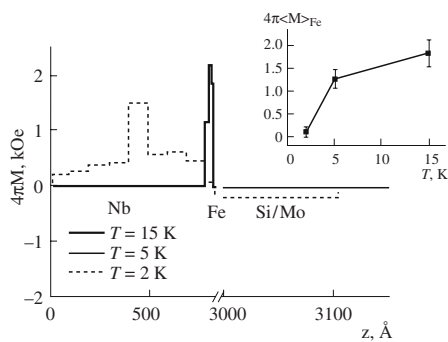


To check whether this difference is related to the superconducting state, it was measured the temperature dependence $S_1(T)$ (Which can be seen in the following figure) using the following protocol. Above T_c , the sample was magnetized to saturation for a short time, and then the field was released to zero, and the sample was cooled down to 3.3 K in zero field. Then a field of $H=661$ Oe was applied, and $S_1(T)$

was measured by first heating the sample to $T = 7$ K [black curve] and then cooling it back in the same field to $T = 3.3$ K [Red curve]. As we can see, the amplitude of S_1 is indeed suppressed below T_c if the sample is cooled in zero field. When analyzing the other two samples, it was observed that the magnitude of the suppression is inversely proportional to d_f . All these observations point to an electro-dynamical origin of the effect. Indeed, for $d_f \sim \xi_f$ two adjacent S layers are expected to be coupled by the proximity effect. This means that the whole sample is a superconductor with a thickness of $D_S = 12D \approx 300\text{nm}$ that is larger than the magnetic screening length $\lambda_{Nb} \sim 120\text{nm}$ in niobium films. Such a thick superconductor can expel a certain amount of external field. Consequently, the central Gd layers feel less of the magnetic field than applied outside; Hence their response is smaller.

The second analyzed structure (which is a non-homogeneous heterostructure) is a more difficult situation. In this case, the structure composition was described as a $x=A/B$ structure, where the fraction of vanadium in a mixture with iron is $A = 0, 0.3, \text{ or } 0.6$, and the type of the intermediate layer between the magnetic layers is $B = V$ or Cr . After performing several neutrons based measurements, there were a few reasonable conclusions to be remarked. The first one would be that the investigations over these structures revealed the specific features of magnetic properties of ferromagnetic–superconducting layers structures. The results over a high temperature of 300K, a low temperature in the range 8–150K, a temperature below 7–8 and 4K, a high field of several kilooersteds, and a low field of about 25Oe should be distinguished. In the temperature range 150-300 K, ferromagnetic clusters are present and ferromagnetic domains are absent. This finding is evidenced by the presence of neutron scattering in a high magnetic field of 9 kOe (clusters) and the absence of neutron scattering with the transfer of a wavevector of $10^{-5} - 10^{-4} \text{ \AA}^{-1}$ (domains 10–100 μm in size) in a low field of about 20 Oe. Ferromagnetic domains appear at temperatures below 150K.

The magnetic behavior of the layered structure with $x=0.3/V$ is as follows. At room temperature, there exist spatially disordered magnetic and nuclear clusters made of Fe, V, Cr, and Nb mixed in various ratios. In the general case, the action of a magnetic field and temperature on the structure's magnetic state is determined by the initial state of a system of clusters. From a temperature of 170K down to the superconducting transition temperature in the niobium layer (6.8K), the moments of clusters 5 and 21 nm in size are frozen, and a ferromagnetic domain state (domain sizes of 250 and 30 μm) forms. Beginning from the superconducting transition temperature in the niobium layer ($T = 6.8\text{K}$) or, even more pronounced, from the superconducting transition temperature in the vanadium layer ($T = 4\text{K}$) to the minimum experimentally achieved temperature (1.5K), the magnetizations of the structures more than 5 nm in size are suppressed by superconductivity, which is thought to be caused by the disordering of the moments of clusters. However, It is not inconceivable, that the absolute value of the magnetic moments of clusters decreases in this case. The structure's magnetic state is relaxed in the magnetic field range from 17Oe to 8kOe, resulting from changes in systems of clusters, domains, and Abrikosov vortices. Last but not least, after studying $Nb(500\text{\AA})/Fe(39\text{\AA})/[Si(34\text{\AA})/Mo(34\text{\AA})]_{40}$ nanostructures, a significant proximity effect came out, which is the inverse effect. In this case, and different from what had been described above, we would describe a little bit of the magnetic's order influence in the ferromagnet over the superconductor's magnetic order. In order to do this, let us take a look at the following figure.



As we can see, this is a magnetization profile of the system at different temperatures, which was formed after the curves of spin asymmetry were fitted by the variation of the magnetization profile $M(z)$ (this data was collected through neutrons based measurements on the system). The variation of the average magnetization of an FM layer with temperature is shown in the insert. The fitting results are described as follows. At $T = 15\text{K}$, only the iron layer with the magnetization of 1.9 ± 0.3 kOe is magnetic.

The mean magnetization of iron decreases down to 1.3 ± 0.2 kOe with a decrease in temperature down to 5K and a small diamagnetic moment of 20Oe appears in the niobium layer. The small value of the diamagnetic moment is related to the fact that the penetration depth of the magnetic field is compared to the thickness of the niobium film. The curve's behavior at $T = 2\text{K}$ was described by the introduction of the magnetic layer 100 \AA thick with a positive magnetization of $1.5 \pm 0.5\text{kOe}$ into the niobium center. The magnetization of the portion of the niobium layer adjacent to this layer is also positive and monotonously decreases from the center to interfaces. The magnetization of the iron layer and Si/No

structure is 0.1 and 0.2kOe, respectively. The appearance of the magnetic field with positive magnetization in niobium at 2K is associated with the formation of a set of Abrikosov vortices. The linear vortex size averaged in the plane is 100\AA , which is correspondingly less than the coherence length in niobium $\xi_{Nb} \sim 400\text{\AA}$.

Project goals

The aim of the work behind this project report was to study the mutual influence of ferromagnetism and superconductivity in the $Al_2O_3 // Nb (100\text{nm}) / Gd (3\text{nm}) / V (70\text{nm}) / Nb (150\text{nm})$ multilayer structure. To observe the inverse proximity effect, particularly. In order to analyze the data collected from the REMUR polarized neutron reflectometer, the followed steps were made. First, to process the experimental data and determine the structure's magnetic profile (spatial distribution of the magnetic field induction), to process the experimental data, these were displayed through Spectraviewer software. Then, in order to model the phenomena, a software, coded in Matlab, based on the Schrodinger equation results for this problem, was used. And at last, to formulate conclusions regarding the implementation of the inverse proximity effect.

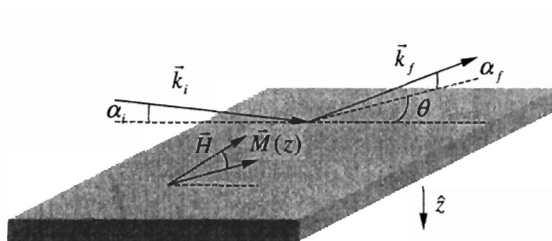
Methods

Description of polarized neutron reflectometry

As it has and will be evident in this report, when getting to understand these S/F systems behaviors, the related neutron measurements are quite important. As we can tell, PNR has been the most potent tool when studying S/F systems so far. It is essential to understand that polarised neutron reflectometry provides enough information so it can be used to measure magnetization profile $J(z)$ (which is one of the fundamental declared goals) and the depth profile of the density of the nuclear neutron scattering length and to determine the nuclear and magnetic structures in the layer plane (plane XY) etc.

Let us take a look at this experimental method's physic principle.

The wave properties of the neutron make possible the optical study of matter by means of neutron beams. As shown in the following figure:



As can be seen, a beam of neutrons is reflected from a flat, laterally homogeneous object. The intensity of the reflected beam, recorded at different neutron wavelengths and angles of incidence, permits an evaluation of the chemical and magnetic depth profile. If the surface is not really homogeneous, the exiting neutron's angles may be different from that of the incoming beam, either in the reflection

plane ($\alpha_i \neq \alpha_r$) or out of it ($\theta \neq 0$), depending on the geometry of the inhomogeneities. The case of specular reflection is the simplest to treat. The neutron's momentum, $|K| = 2\pi/\lambda$ (where λ is the neutron wavelength), can be separated into two components, parallel and perpendicular to the surface. Only the perpendicular component is altered by the potential $U(z)$ describing the laterally homogeneous material. Thus, we can represent the neutron as a particle with kinetic energy $\hbar^2 K_z^2/2m$, hitting a potential of height $U(z)$. If its energy is too low, the neutron bounces back. A part of the potential, which is present in all matter, is simply related to the scattering length (b) of the N constituent nuclei per unit volume: $U_z = (\hbar^2/2m)N(z)b(z)$. For thermal and cold neutrons, the isotopic b is constant and conveniently tabulated for all nuclei (as well as for all element's natural isotopic composition). In free space (above the surface) $U(z)$ is similar to zero, and the neutron wave function is $u(z) = \exp(ik_z z) + r \exp(-ik_z z)$ for a plane wave incident on the surface from above. The wave function inside the material is linked to the potential by the *Schrödinger* equation, whose solution gives the reflectance r . In a scattering experiment, the observed quantity is the reflectivity $R = |r|^2$.

The wave vector transfer $Q_z = k_{zf} - k_{zi} = 4\pi \sin(\alpha)/\lambda$ provides a convenient metric for characterizing the specular reflection process in which incident- and reflected-beam wave vectors (\vec{k}_i, \vec{k}_f) enter and exit the surface at the same glancing angle α . Since momentum $\hbar Q_z$ is the quantum mechanical conjugate to position z , one can transform the depth profile of scattering material $b(z)$ into reflectivity $R(Q_z)$. The inverse process (from reflectivity to profile) is more complicated. However, some simple rules give a flavor of the link between two quantities.

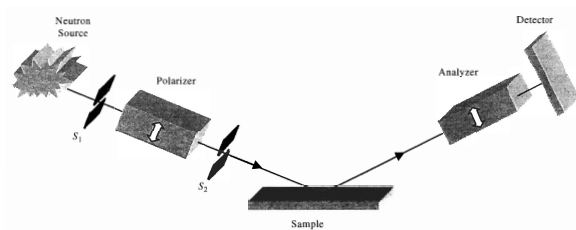
In general, the reflectivity is unitary for most material up to a value of $Q_c = \sqrt{16\pi N b}$ of order 0.01 \AA^{-1} . Beyond this limit, the reflectivity decreases rapidly with a mean asymptotic Q_z^{-4} dependence. For $Q_z \gg Q_c$, the reflectivity from a sequence of L layers is well described by using the first Born approximation:

$$R \approx |4\pi \sum_{l=1} [(Nb)_l - (Nb)_{l-1}] \exp(iQ_z d_l)|^2 / Q_z^2, \text{ where } d_l \text{ is the distance of the } l\text{th layer's}$$

top interface below the surface. Neutron also interacts with the magnetic induction field \vec{B} . In the presence of magnetic induction, the interaction potential is described by the following expression $U(z) = U_n(z) + U_m(z) = \hbar N(z)b(z)/2m + \vec{B} \hat{s}$, where \hat{s} is the neutron spin operator. Since the neutron is a $-1/2$ spin particle, there are two states of quantization concerning an external magnetic field \vec{H} . In measurement, the neutron may be polarized either parallel (+) or antiparallel (-) to \vec{H} . So if we suppose that the neutron is polarized in an applied field \vec{H}_p . Upon encountering and induction \vec{B}_s with a different orientation (for instance, inside a sample), the neutron changes its spin state. In classical terms, the neutron

moment processes about \vec{B}_s . The final neutron state may be analyzed in terms of the polarization concerning to a third field, \vec{H}_a . If, as is customarily done, $\vec{H}_a \parallel \vec{H}_p$, four reflectivity's can be measured like $R^{++}, R^{+-}, R^{-+}, R^{--}$. On the other hand, a polarized neutron beam incident on a ferromagnetic layer aligned parallel to an external field exhibits no specular spin flip scattering. However, an in-plane ferromagnetic layer's orientation can be determined by measuring the spin-flip's intensity relative to non spin-flip scattering.

In the case of the instrument description and use modes, let us say that a reflectometer is a simples instrument. A neutron beam of wavelength lambda strikes a sample surface at angle α_i and is reflected from the surface at α_f as it is noticeable in the following figure.



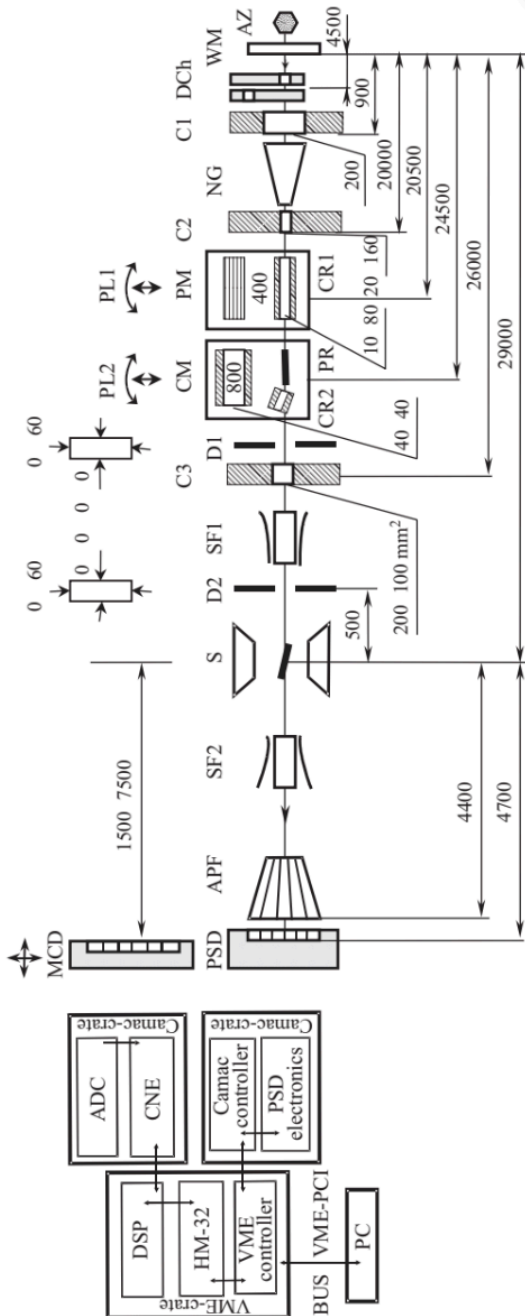
The instrument functions as a diffractometer with resolution sufficient to separate transmitter and reflected beams at values Q_z near where the reflectivity becomes unitary. Specular reflectivity ($\alpha_i = \alpha_f$) is solely a function of the momentum transfer along the

\hat{z} direction. Hence ,in practice, a range of Q_z is spanned either by changing the wavelength and keeping fixed the angle of incidence or changing the angle of incidence at a fixed wavelength. Appropriate devices, such as polarising mirrors and flat coil spin-flippers, polarize the incoming neutrons along an applied magnetic field or analyze the reflected beam's polarization. Conventionally, the direction of the initial polarization is fixed. The sample may change the neutron's polarization, and an analyzer chooses, among the reflected neutrons, those aligned with the polarizer. The reversal of the neutron's spin is obtained by energizing flippers before and after the sample. The reflectivities are then characterized by the neutron polarization sign before and after reflection concerning the reference field $R^{++}, R^{+-}, R^{-+}, R^{--}$.

Description of REMUR spectrometer and its relation with secondary radiation measurements.

THE FUNCTIONAL SCHEME OF THE SPECTROMETER

In the polarized neutron spectrometer REMUR, there is realized:



- 1. Mode to measure the reflection of polarized neutrons and their transmission through a layered structure (reflectometric mode), and the mode to measure diffuse small-angle neutron scattering (small-angle mode).
- 2. Complete polarization analysis of the reflected and the scattered neutron beam allows the investigation of processes with/without a change in the neutron spin state.
- 3. Polarization analysis of the neutron beam concerning the local field in the investigated sample based on the effect of the neutron beam's spatial splitting occurs if there is a nonzero probability of neutron transition between spin states.
- 4. Position-sensitive detection of neutrons with the angular resolution in the horizontal plane ± 0.17 mrad.
- 5. Shifting of the polarization efficiency of the reflectometric mode in the neutron wavelength interval $1.5 \div 5 \text{ \AA}$ accomplished by changing the glancing angle of the neutron beam falling on the upper mirror of the neutron polarizer.
- 6. Automated switching over the spectrometer's state during its operation in a specified mode, automated acquisition of the spectrometric data, control of the state of individual blocks of the spectrometer.
- 7. Visualization and express-analysis of the spectrometric data.

On other hand, as it has been know, neutron reflectometry is a method for measuring the spatial dependence (profile) of the potential interaction between neutron and medium. At the interface of media, the interaction potential is the sum of the element's potentials. For the definition of potentials of separate elements (isotopes), secondary radiation is recorded. Recording secondary radiation channels are created on spectrometer REMUR at pulsed reactor IBR-2 in Dubna (Russia).

The properties of interface regions significantly change in a layered structure. So, for the superconductor-ferromagnetic interface, there is a modification of the magnetic spatial profile. At that, a question is how relates the magnetic profile with element density profiles. Polarized neutron reflectometry allows measuring the spatial profile of magnetic induction. The neutron-matter interaction potential (proportional to magnetic induction) is the sum of potentials of the interacting environment. So, conventional reflectometry can not say what the elements are responsible for changing the potential. For that, a secondary radiation must be recorded. The type of radiation and energy of these are signs that allow you to identify the isotopes of elements. Secondary radiation is constituted by charged particles, gamma-quanta, and nuclear fission fragments. A more broad interpretation of secondary radiation relates relate non-coherent scattering on nuclear, inelastic, and diffuse neutron scattering. The particular secondary radiation is the spin-flip neutrons.

Channels for recording the secondary radiation are created at spectrometer polarized neutrons REMUR located at the IBR-2 pulsed reactor in Dubna (Russia). IBR-2 reactor, which operates with a frequency of 5Gz. Spectrometer REMUR has the next basic parameters; distance from sample place to the moderator is 29 meters, distance from the sample place to neutron detector is 5 meters, the wavelength resolution at detector place is $\delta\lambda=0.02\text{\AA}$.

In order to measure this secondary radiation, a particle channel register was used. It was essential to use an ionization chamber for the registration of the charged particles. Inside of the ionization chamber, there are placed the layered structures you want to investigate. Layered structures included neutron absorption layers $6\text{Li}0.97\text{Li}0.1\text{F}(5\text{nm})$. On the other hand, in order to register gamma quanta, it was used a gamma channel, which is defined by the usage of a semiconductor germanium detector with efficiency 45% and energy resolution 2Kev for line 1.33 Mev.

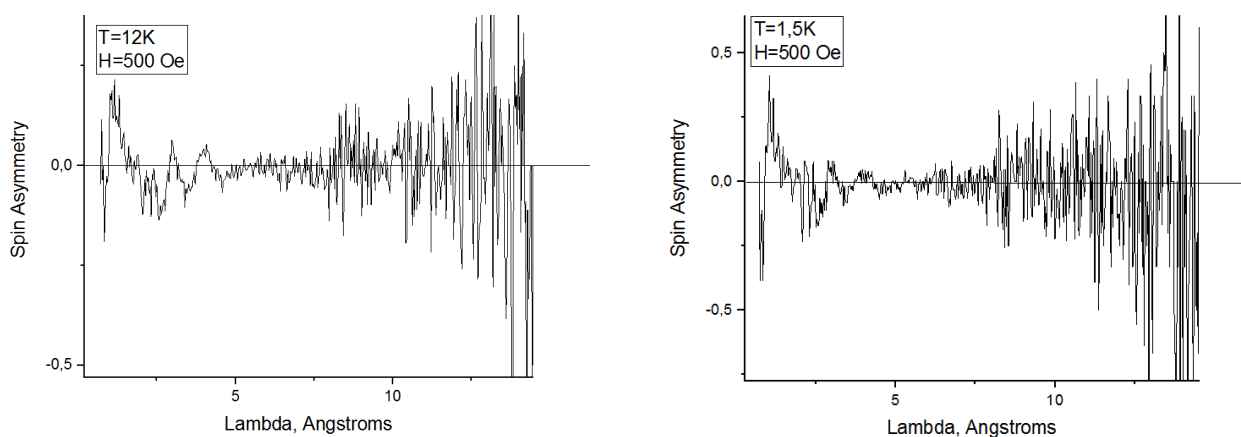
In real-time, at the neutron spectrometer REMUR, enough many isotopes are available for secondary radiation registration measurements. Further progress is connected with increasing neutron intensity 10 times, decreasing fast neutrons' background and gamma radiation from active reactor zone 4-10 times, increasing the gamma detector solid angle 4-5 times. Together using of these measures will allow the detection to reach $\sigma_{min} \approx 11\text{mbarn}$ at $h \approx 5\text{nm}$ or 1\AA at $\sigma_{min} = 50\text{mbarn}$. With a super mirror reflector, it can be achieved a spatial resolution of 1\AA also.

Results

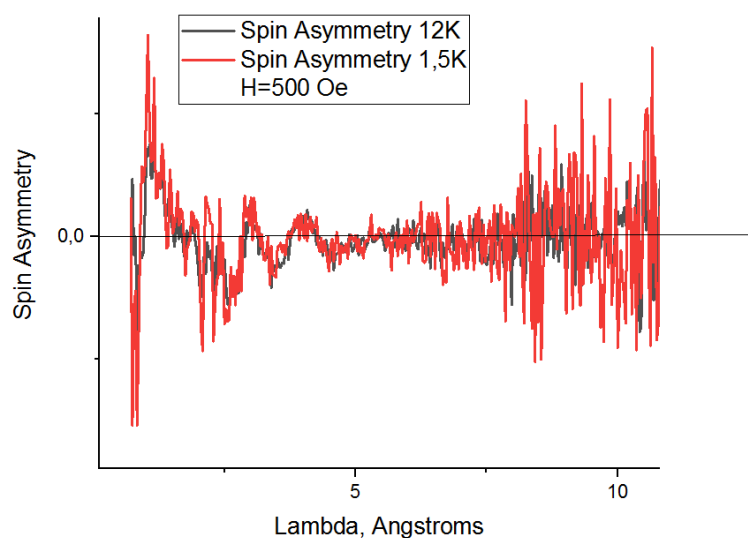
When studying the structure (which is composed by the following set of layers ($Nb_1, V_1, V_2, Gd, Nb_2, Nb_3, AL_2O_3$)) several neutron measurements were performed. It is important to detail the followed protocol in order to be able to imagine the process and to guide us through the results.

First of all, the structure, under the presence of an external magnetic field of intensity $H=20$ Oe was cooled down from 300K to $T=12$ K. It was followed by an increase in the external magnetic field's intensity that reached a value of $H=1.9$ Koe at $T=12$ K (this magnetic field was sustained for one minute). Once the minute was passed, the external field's intensity decreased to a value of $H=500$ Oe. Later, under these conditions, a set of measurements were performed at $T=12$ K. Then, the system's temperature decreased from 12K to 1.5K and a set of measurements were performed at $T=1.5$ K.

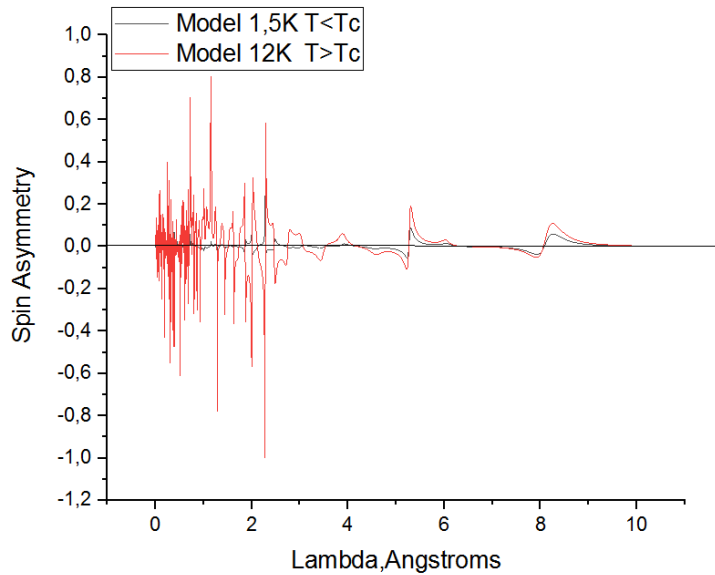
Let us take a look to the following graphs, which shows the neutron spin asymmetry based on the collected information from experimental measurements.



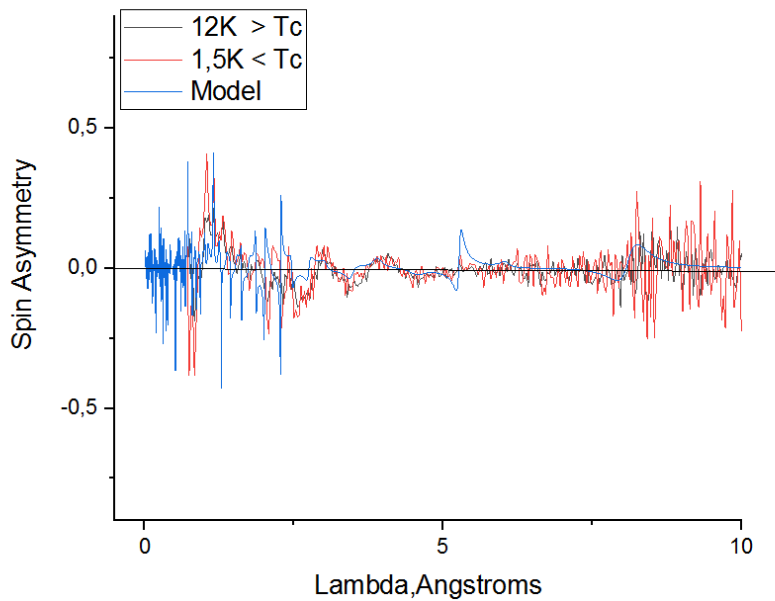
If we compare both behaviors we would acquire the following information:



On the other hand, if we model the problem, and solve the Schrodinger equation for this particular system and these particular conditions, we would obtain the following behaviors above and below T_c :



Then when we compare it with the results that were achieved through the experimental data, we would obtain the following:



Conclusion (discussions, perspectives)

In the first part of the results we can observe a very significant difference in the reported values of Spin asymmetry with the same neutron wavelengths. This is because of the existence of the inverse proximity effect, which takes place through the magnetization of the Superconductor because of the action of the Ferromagnet over it. In the second part of the results, we can see differences between the Spin asymmetry reported by the model (which is supported and developed under the idea of the existence of these proximity effects) when the measurement temperatures changes from above to below T_c . In the last part of the results it is noticeable a certain deviation between the behavior of a system which is expressed by experimental and theoretical manners respectively. These differences could be well influenced by the fact that during the model's setup, a neglective decision was made regarding non-collinear scattering. However the similarity could be improved through an iterative changing of initial conditions.

I must say that this phenomena is quite interesting and I think that its scope could be expanded through the study of other structures and by changing the measurement's protocols. Maybe this proximity effects could be used as a controller of the magnetic field intensity when trying to direct charged particles beams, or maybe it could be useful if it is intended to perform low temperature measurements, so, this proximity effects and material science could help to decreased in a controlled way the inducted magnetic field or the superconductor's action over the studied system.

Acknowledgements

I would like to thank to JNIR (Joint Institute for Nuclear Research) for this Remote student training which has been exquisitely interesting. I would like to thank my supervisor Vladimir Zhaketov also, for his hard work on it and his patience while teaching me part of the knowledge that he has acquire through the years, while he has been studying these very interesting proximity effects. I would like to thank Profesor Cesar García Trápaga from the Superior Institute of Technologies and Applied Sciences of Cuba (which is my current school) for inviting me to apply for this Remote student training also.

References

- 1- “Magnetic proximity effect in Nb/Gd superlattices seen by neutron reflectometry”. Yu. N. Khaydukov, E.A. Kravtsov, V. D. Zhaketov, V. V. Progliado, G. Kim, Yu. V. Nikitenko, T. Keller, V. V. Ustinov, V. L. Aksenov, and B. Keimer.
- 2- “Coexistence of Superconductivity and Ferromagnetism in the Nb(500 Å)/Fe(39 Å)[Si(34 Å)/Mo(34 Å)]₄₀/Si Nanostructure”. V. L. Aksenov, Yu. V. Nikitenko, Yu. N. Khaidukova, S. N. Vdovichev, M. M. Borisov, A. N. Morkovin and E. Kh. Mukhamedzhanov.
- 3- “Magnetism in Structures with Ferromagnetic and Superconducting Layers”. V. D. Zhaketov a , Yu. V. Nikitenko, F. Radu , A. V. Petrenko , A. Csik, M. M. Borisov, E. Kh. Mukhamedzhanov , and V. L. Aksenov.
- 4- “Polarized Neutron Reflectometry”. J.F. Ankner and G.P Felcher.
- 5- “The polarized Neutron Spectrometer REMUR at the pulsed Reactor IBR-2”. V. L. Aksenov, K. N. Jernenkov, S. V. Kozhevnikov, H. Lauter, V. Lauter-Pasyuk, Yu. V. Nikitenko, A. V. Petrenko.
- 6- “Reflectometry with registration pf secondary radiation at local neutron reflection”. V. D. Zhaketov, A. Petrenko, Yu. N. Kopatch, N. A. Gundorin, C. Hramko, Yu. M. Gledenov, Yu. V. Nikitenko, V. L. Aksenov.